This article has been accepted for inclusion in a future issue of this journal. Content is final as presented, with the exception of pagination.

The Complexity in Complete Graphic Characterizations of Multiagent Controllability

Zhijian Ji, *Senior Member, IEEE*, Hai Lin, *Senior Member, IEEE*, Shaobin Cao, Qingyuan Qi, and Huizi Ma

***Abstract*—Establishing the graph-based criterion for the selection of any location and any number of leaders is the main difficulty in the complete graphic characterization of multiagent controllability. This greatly increases the complexity of the study, compared with the results derived for only one or several classes of leaders. Through a detailed analysis of graphs of six nodes, this article presents a systematic design and identification process for the complete graphic characterization by taking advantage of controllability destructive nodes. The topologies obtained by the proposed method allow directly determining controllability at the network topology level. The results are not only applicable to any leader's selection but also reveal the difficulty and complexity in the study of complete controllability graphic characterizations. Moreover, by comparing graphs composed of five and six nodes, the results reveal the graph-theory-based controllability complexity caused by adding only one node. Finally, results are derived to show how to design topology structures to ensure the controllability under any selection of leaders.**

***Index Terms*—Complete graphic characterization, destructive nodes, local interactions, multiagent systems, topology structure.**

I. Introduction

THE STUDY of multiagent controllability has two aspects: one is to build results against any graph for the selection of one or several kinds of leaders and the other is to derive results for the selection of any leader in graphs consisting of a fixed number of nodes. Although the latter question is not simpler than the previous one, its investigation has not attracted as much attention as the previous one (e.g., [1]–[17]). Here, we combine the latter to study the complexity in controllability.

Manuscript received August 6, 2019; revised December 1, 2019; accepted February 4, 2020. This work was supported in part by the National Natural Science Foundation of China under Grant 61873136, Grant 61903210, and Grant 61603288, and in part by the Science Foundation of Shandong Province for Distinguished Young Scholars under Grant JQ201419. This article was recommended by Associate Editor L. Zhang. *(Corresponding author: Zhijian Ji.)*

Zhijian Ji, Shaobin Cao, and Qingyuan Qi are with the Institute of Complexity Science, College of Automation, Qingdao University, Qingdao 266071, China (e-mail: jizhijian@pku.org.cn; csbin2016@163.com; qiqy123@163.com).

Hai Lin is with the Department of Electrical Engineering, University of Notre Dame, Notre Dame, IN 46556 USA (e-mail: hlin1@nd.edu).

Huizi Ma is with the College of Mathematics and Systems Science, Shandong University of Science and Technology, Qingdao 266590, China (e-mail: helenmahuizi@163.com).

Color versions of one or more of the figures in this article are available online at http://ieeexplore.ieee.org.

Digital Object Identifier 10.1109/TCYB.2020.2972403

The number and positions of leaders are two factors that lead to the complexity. Even for a graph consisting of a fixed number of nodes, the topology structure of the follower subgraph varies with the leaders choice. That is why there are 1050 kinds of topologies that need to be considered for the graphs consisting of only five nodes [18]. Since controllability relates closely with the topology structures, the graph-theoretic characterization of multiagent controllability is far from solved because the reported results do not cover all leaders selection scenarios. This inspires here the investigation of complete graphic characterization for controllability, which refers to determining controllability directly from the topology structures of graphs. The word "complete" means that the proposed determination is applicable to any leader selection for any given graph. Thus, the associated controllability can be determined directly from the identified controllability destructive topologies. To this end, we will dig out all controllability destructive topologies according to the selection of all leaders. The controllability is then determined as whether the graph contains a controllability destructive structure and a system is controllable if and only if the graph does not contain any destructive topology structure.

It is extremely difficult to identify all controllability destructive topologies because one has to face too many topologies to authenticate. For example, for each graph of six nodes, there are $\sum_{i=1}^{5} C_6^i = 62$ ways of leaders selection. Since there are 112 different topologies in the six-node graph, there are 6944 types of topologies resulting from the selection of all leaders. This number contrasts sharply to the number of nodes 6. How to identify all of the controllability destructive structures from these topologies is a challenging problem.

Although there are many results about controllability, consensusability, and the associated distributed protocols (e.g., [19]–[40]), none of them can fully answer the controllability of all the above topologies, even if these graphs all contain the same number, say six vertices. A large number of controllability questions remain unanswered in relation to other leaders selection (e.g., [41]–[56]). Recently, it was shown that controllability can be studied from the viewpoint of controllability destructive nodes [18]; however, there is still a lack of systematic method based on this concept. In addition, to have a deeper perception of the complexity, there should be a comparison between at least two types of graphs, say, a six-node and a five-node graph. We will show that even with a single node difference, the difference in controllability

2168-2267 © 2020 IEEE. Personal use is permitted, but republication/redistribution requires IEEE permission.
See https://www.ieee.org/publications/rights/index.html for more information.

Authorized licensed use limited to: Qingdao University. Downloaded on September 27,2020 at 09:14:25 UTC from IEEE Xplore. Restrictions apply.

This article has been accepted for inclusion in a future issue of this journal. Content is final as presented, with the exception of pagination.

complexity between the two types of graphs is huge. This is because the additional node makes one have to consider the destructive topologies consisting of five vertices, which, however, does not need to be studied for five-node graphs. Beyond that, in the graphs of six nodes, the topology structures of double, triple, and quadruple destructive nodes are much more complicated than those in five-node graphs. So new technical details need to be developed to deal with the emerging circumstances. The contributions of this article are given as follows.

1) We show that even if there is only one node difference in the number of nodes that make up the graph, the specific study varies greatly because just one-node difference will make the leaders selection greatly different. By a detailed interpretation of the six-node graph, we not only give the specific process of obtaining the complete graphic characterization but also exhibit the situation one has to face to obtain the characterization.
2) By identifying controllability destructive nodes, the factors causing the complexity are analyzed in detail. The proposed design steps indicate that each additional node in the graph at least doubles the complexity. This growing trend in complexity is revealed for the first time.
3) A general design process is proposed for characterizing the graphic controllability, by which the complexity is quantitatively described. This, together with [18], presents for the first time a comparatively intact picture of the complete graphic controllability characterization.
4) A necessary and sufficient condition is derived for the essential controllability, and a step-by-step design procedure is proposed to construct graphs with essential controllability.

The remainder of this article is given as follows. In Section II, basic concepts are given. In Section III, we propose specific implementation steps by using the identified controllability destructive topologies to fully characterize the graphic features of controllability. In Section IV, essentially controllable graphs are revealed. The conclusion is given in Section V.

II. Preliminaries

Consider a set of $n+l$ single-integrator agents given by

$$\begin{cases} \dot{x}_i = u_i, & i = 1, \ldots, n \\ \dot{z}_j = u_{n+j}, & j = 1, \ldots, l \end{cases} \tag{1}$$

where n and l are the number of followers and leaders, respectively; and x_i and z_j are the states of the ith and $(n+j)$th agent, respectively. Let $z_1, \ldots, z_l$ act as leaders and be influenced only via external control inputs. $\mathcal{N}_i = \{j \mid v_i \sim v_j; j \neq i\}$ represents the neighboring set of v_i and "$\sim$" denotes the neighboring relation. The followers are governed by the neighbor-based rule

$$u_i = \sum_{j \in \mathcal{N}_i} (x_j - x_i) + \sum_{(n+j) \in \mathcal{N}_i} (z_j - x_i) \tag{2}$$

where $j \in \{1, \ldots, n\}$; and $(n+j) \in \{n+1, \ldots, n+l\}$. x and z denote the stack vectors of x_is and z_js, respectively. The information flow between agents is incorporated in graph $\mathcal{G}$, which consists of a node set $\mathcal{V} = \{v_1, \ldots, v_{n+l}\}$ and an edge set $\mathcal{E} = \{(v_i, v_j) \in \mathcal{V} \times \mathcal{V} \mid v_i \sim v_j\}$, with nodes representing agents and edges indicating the interconnections between them. $\mathcal{L} = D - A$ is the Laplacian, where A is the adjacency matrix of $\mathcal{G}$ and D is the diagonal matrix with diagonal entries $d_i = |\mathcal{N}_i|$, the cardinality of $\mathcal{N}_i$. Under (2), the followers' dynamics is

$$\dot{x} = -\mathcal{F}x - \mathcal{R}z \tag{3}$$

where $\mathcal{F}$ is obtained from $\mathcal{L}$ after deleting the last l rows and l columns; and $\mathcal{R}$ consists of the first n elements of the deleted columns. Since (3) captures the followers' dynamics, the controllability of a multiagent system can be realized through (3). A path of $\mathcal{G}$ is a sequence of consecutive edges. $\mathcal{G}$ is connected if there is a path between any distinct nodes. A subgraph of $\mathcal{G}$ is a graph whose vertex set is a subset of $\mathcal{V}$ and whose edge set is a subset of $\mathcal{E}$ restricted to this subset. A subgraph is induced from $\mathcal{G}$ if it is obtained by deleting a subset of nodes and all the edges connected to those nodes. An induced subgraph, which is maximal and connected, is said to be a connected component. Controllability can be studied under the assumption that $\mathcal{G}$ is connected [48]. Let agents $n+1, \ldots, n+l$ play leaders' role. Define

$$\mathcal{N}_{kf} \triangleq \{i | v_i \sim v_k, v_i \text{ is a node of follower subgraph } \mathcal{G}_f\}$$
$$\mathcal{N}_{kl} \triangleq \{j | v_j \sim v_k, v_j \text{ is a node of leader subgraph } \mathcal{G}_l\}.$$

Then, $\mathcal{N}_k = \mathcal{N}_{kf} \cup \mathcal{N}_{kl}$ and $\mathcal{N}_{kf} \cap \mathcal{N}_{kl} = \Phi$, where Φ is the empty set. This partition of neighboring set plays an important role in the derivation of subsequent results.

III. Complexity Analysis and Destructive Nodes

The complexity of characterizing controllability is studied by discriminating controllability destructive nodes.

A. Double, Triple, and Quadruple Destructive Nodes

Definition 1 [18]: v_p, v_q (v_p, v_q, v_r) are said to be double (triple) controllability destructive [DCD(TCD)] nodes if for any v_k other than v_p, v_q (v_p, v_q, v_r), $\mathcal{N}_{kf}$ contains either both p and q (all p, q, r) or neither (none) of them.

Although DCD and TCD nodes happen to be defined in the same way, which cannot be generalized to the quadruple controllability destructive (QCD) node, the latter is much more complicated and its structure cannot be described in a uniform way. This section will explain step by step that 2068 candidate topologies need to be identified to dig out all of the QCD nodes, despite these 2068 topologies being already prescreened by a proposed method.

1) Preliminary Result: We recall the eigencondition (4) which is from $\mathcal{L}\bar{y} = \lambda\bar{y}$

$$d_k y_k - \sum_{i \in \mathcal{N}_k} y_i = \lambda y_k, \quad k = 1, \ldots, n+l. \tag{4}$$

Consider an eigenvector $\bar{y}$ of $\mathcal{L}$ with $\bar{y} = [0, \ldots, y_{s_1}, \ldots, y_{s_2}, \ldots, y_{t_1}, \ldots, y_{t_2}, \ldots, 0]^T$, $y_{s_1}, y_{s_2}, y_{t_1}, y_{t_2} \neq 0$ and all the other elements being zero. Each entry of $\bar{y}$ ought to satisfy the eigencondition (4). For each $k \neq s_1, s_2, t_1, t_2$; $\mathcal{N}_{kf}$ has the following five cases:

Authorized licensed use limited to: Qingdao University. Downloaded on September 27,2020 at 09:14:25 UTC from IEEE Xplore. Restrictions apply.

This article has been accepted for inclusion in a future issue of this journal. Content is final as presented, with the exception of pagination.

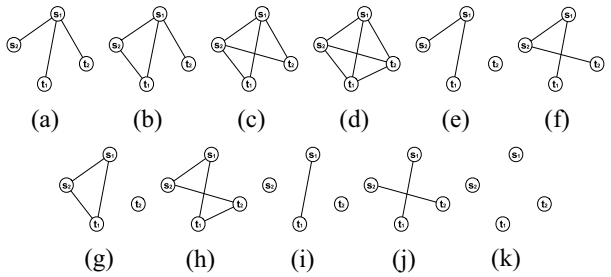

Fig. 1. All topology structures consisting of s_1, s_2, t_1, and t_2.

1) $s_1, s_2, t_1, t_2 \in \mathcal{N}_{kf}$;
2) any three and only three of s_1, s_2, t_1, t_2 belong to $\mathcal{N}_{kf}$;
3) any two and only two of s_1, s_2, t_1, t_2 belong to $\mathcal{N}_{kf}$;
4) any one and only one of s_1, s_2, t_1, t_2 belongs to $\mathcal{N}_{kf}$;
5) none of s_1, s_2, t_1, t_2 belongs to $\mathcal{N}_{kf}$.

Proposition 1 [18]: Assuming leaders are selected from $\mathcal{V} \setminus \{v_{s_1}, v_{s_2}, v_{t_1}, v_{t_2}\}$ and $\bar{y}$ is an eigenvector of $\mathcal{L}$, then:

1) for any given $k \neq s_1, s_2, t_1, t_2$; $\mathcal{N}_{kf}$ falls into one and only one of the following two situations:
   a) at least one of cases 1), 3), and 5) occurs;
   b) at least one of cases 2), 3), and 5) occurs.

   Moreover, if 2) arises, there are at most three different $k \neq s_1, s_2, t_1, t_2$ with each $\mathcal{N}_{kf}$ containing a different set of three indices of $\{s_1, s_2, t_1, t_2\}$; and so does 3) with each set containing two indices of $\{s_1, s_2, t_1, t_2\}$;
2) for $k = s_1, s_2, t_1, t_2$, all possible topologies consisting of $v_{s_1}, v_{s_2}, v_{t_1}, v_{t_2}$ are depicted in Fig. 1.

Proposition 1 greatly reduces the number of graphs to 2068 required in the identification of QCD nodes, as will be explained in more detail as follows.

Definition 2: A graph is said to be designed from (a) of Fig. 1 if the topology structure of $v_{s_1}, v_{s_2}, v_{t_1}, v_{t_2}$ is in accordance with (a) and the graph is obtained by adding edges between $\{v_{s_1}, v_{s_2}, v_{t_1}, v_{t_2}\}$ and $\mathcal{V} \setminus \{v_{s_1}, v_{s_2}, v_{t_1}, v_{t_2}\}$.

Definition 2 applies to other topologies of Fig. 1.

2) Design of Candidate QCD Nodes: This section is devoted to the design of candidate QCD nodes topologies for identification. Let us relabel $v_{s_1} = v_5, v_{s_2} = v_3, v_{t_1} = v_4$, and $v_{t_2} = v_6$. The six nodes are divided into $\{v_1, v_2\}$ and $\{v_3, v_4, v_5, v_6\}$. Nodes v_3–v_6 form 11 different topologies as shown in Fig. 1, and v_1 and v_2 form two different topologies

$$\Xi \triangleq \begin{cases} \text{(a) two isolated nodes} \\ \text{(b) a line segment connecting } v_1, v_2. \end{cases}$$

Combining (b) of Ξ with (f) of Fig. 1 yields graph (a) of Fig. 2. A total of 22 such graphs can be generated by combining topologies of Ξ with those of Fig. 1. The remaining ones use Propositon 1 to design information flow between $\{v_1, v_2\}$ and $\{v_3, v_4, v_5, v_6\}$. Let us focus on Fig. 2(a). It is the original graph in which the information flow between $\{v_1, v_2\}$ and $\{v_3, v_4, v_5, v_6\}$ is to be designed. The other 21 graphs can be analyzed the same way. By Propositon 1, there are subsequent circumstances in identifying candidate QCD nodes.

1) At least one case of 1), 3), and 5) occurs. More specifically, they are given in the following.
   a) Case 1) occurs on only one of v_1 and v_2, say v_2 in graph (b) of Fig. 2, and case 5) occurs on v_1.
   b) Case 1) occurs on only one of v_1 and v_2, say v_2 in graphs (b)–(h) of Fig. 2 and case 3) occurs on v_1.
   c) Case 1) occurs on both nodes v_1 and v_2. This situation corresponds to graph (i) of Fig. 2.
2) At least one of cases 2), 3), and 5) occurs.
   a) Case 2) occurs on only one of nodes v_1 and v_2, say v_2 here and case 5) occurs on v_1. The corresponding graphs are (a)–(d) of Fig. 3.
   b) Case 2) occurs on both v_1 and v_2. In this situation, graphs (e)–(h) of Fig. 3 correspond to (a) of Fig. 3.
   c) Case 2) occurs on v_2 and case 3) occurs on v_1.
   d) Case 3) occurs only on v_2. The corresponding topologies are depicted in Fig. 4.
   e) Case 3) occurs on both v_1 and v_2. Thus, graphs (a)–(f) of Fig. 5 are designed from (a) of Fig. 4 by applying case 3) on v_1. Similarly, Figs. 6–10 are, respectively, designed from (b)–(f) of Fig. 4.

Topologies designed from case 1) are depicted in Fig. 2.

There are 44 topologies designed from case 2).

Other cases can be constructed in the same way. Specifically, four graphs are designed from (b) of Fig. 3 by applying case 2) on v_1. The number of graphs designed from (c) of Fig. 3 by applying case 2) on v_1 is also 4, and so are the number of graphs designed from (d) of Fig. 3. There are six topology structures of candidate QCD nodes, which are designed from (a) of Fig. 3 by applying case 3) on node v_1. For each of the following three scenarios, the number of topologies of candidate QCD nodes is also 6: those designed

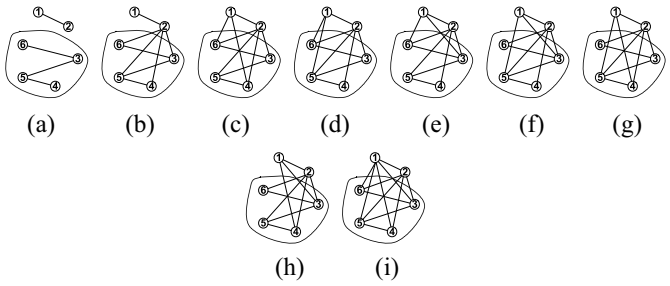

Fig. 2. (a) is the original graph. (b)–(h) are designed by applying case 1) to one of v_1 and v_2 (say v_2), where (b), and (c) to (h) are designed by applying, respectively, cases 5) and 3) to v_1. Graph (i) is designed by applying case 1) to v_1 and v_2. Graphs (b)–(i) are topologies of candidate QCD nodes.

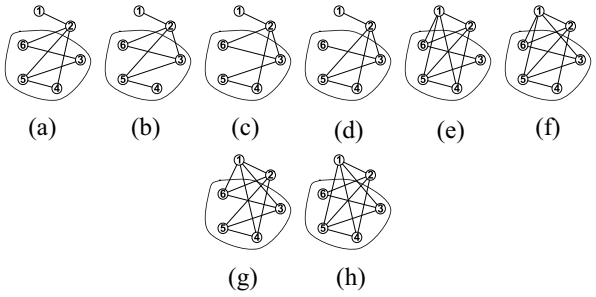

Fig. 3. (a)–(d) are designed by applying case 2) on v_2 and case 5) on v_1. (e)–(h) are designed from (a) by applying case 2) on v_1. They are all topologies of candidate QCD nodes.

Authorized licensed use limited to: Qingdao University. Downloaded on September 27,2020 at 09:14:25 UTC from IEEE Xplore. Restrictions apply.

This article has been accepted for inclusion in a future issue of this journal. Content is final as presented, with the exception of pagination.

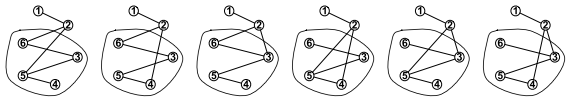

Fig. 4. Topology structures of candidate QCD nodes, which are designed from (a) of Fig. 2 by applying case 3) on only node v_2.

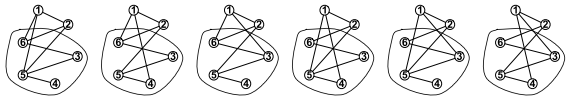

Fig. 5. Topology structures of candidate QCD nodes, which are designed from (a) of Fig. 4 by applying case 3) on v_1.

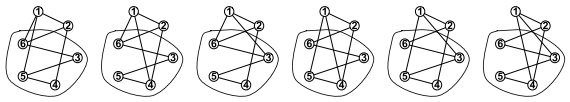

Fig. 6. Topology structures of candidate QCD nodes, which are designed from (b) of Fig. 4 by applying case 3) on v_1.

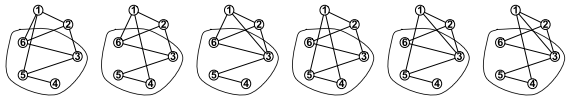

Fig. 7. Topology structures of candidate QCD nodes, which are designed from (c) of Fig. 4 by applying case 3) on v_1.

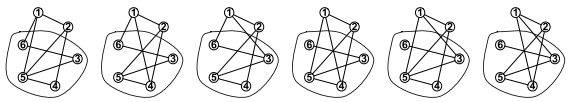

Fig. 8. Topology structures of candidate QCD nodes, which are designed from (d) of Fig. 4 by applying case 3) on v_1.

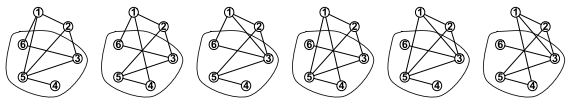

Fig. 9. Topology structures of candidate QCD nodes, which are designed from (e) of Fig. 4 by applying case 3) on v_1.

from (b) of Fig. 3 by applying case 3) on node v_1; designed from (c) of Fig. 3 by applying case 3) on node v_1; and those designed from (d) of Fig. 3 by applying case 3) on node v_1.

The remaining topologies are designed from case 3).

3) Identification: Consider the aforementioned $\bar{y}$. Since (f) of Fig. 1 corresponds to the topology formed by v_3, v_4, v_5, v_6 in (a) of Fig. 2, the corresponding relationship between indices of these two graphs is $t_1 = 6, t_2 = 4, s_1 = 3$, and $s_2 = 5$.

Lemma 1: Suppose $\bar{y}$ is an eigenvector of a graph designed from (f) of Fig. 1. The following assertions hold:

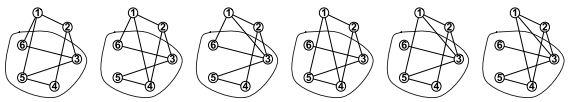

Fig. 10. Topology structures of candidate QCD nodes, which are designed from (f) of Fig. 4 by applying case 3) on v_1.

1) if situation a) of Proposition 1 arises, the associated eigenvalue λ should satisfy the following equation:

$$\begin{aligned} &a_0 + a_1\lambda + a_2\lambda^2 - \lambda^3 = 0 \\ &a_0 \triangleq \big[d_{t_1}\big(d_{s_1} - 1\big) - 2\big]\big(d_{t_2} + 1\big) - \big(2d_{t_2} + 1\big)\big(d_{t_1} + 1\big) \\ &a_1 \triangleq \big(2d_{t_2} + 1\big) + 2\big(d_{t_1} + 1\big) - \big[d_{t_1}\big(d_{s_1} - 1\big) - 2\big] \\ &\qquad - \big[d_{t_1} + \big(d_{s_1} - 1\big)\big]\big(d_{t_2} + 1\big) \\ &a_2 \triangleq \big[d_{t_1} + \big(d_{s_1} - 1\big)\big] + \big(d_{t_2} + 1\big) - 2 \end{aligned} \tag{5}$$

2) if situation b) arises with $v_k \in \mathcal{V} \setminus \{v_{s_1}, v_{s_2}, v_{t_1}, v_{t_2}\}$ incident to only three of $v_{s_1}, v_{s_2}, v_{t_1}, v_{t_2}$, say $v_{s_1}, v_{s_2}, v_{t_1}$, then the nonzero entries of $\bar{y}$ take the following values:

$$\begin{aligned} &y_{s_1} = 1 \cdot k \\ &y_{t_1} = \frac{1}{d_{t_1} - d_{s_1} - 1} \cdot k, y_{s_2} = -1 - \frac{1}{d_{t_1} - d_{s_1} - 1} \cdot k \\ &y_{t_2} = -1 - \big(d_{s_2} - d_{s_1} - 1\big)\left(1 + \frac{1}{d_{t_1} - d_{s_1} - 1}\right) \cdot k \end{aligned}$$

where $k \neq 0$ is an arbitrary real number given in advance. In this case, $\lambda = d_{s_1} + 1$;

3) if situation c) arises with $v_k \in \mathcal{V} \setminus \{v_{s_1}, v_{s_2}, v_{t_1}, v_{t_2}\}$ incident to only two of $v_{s_1}, v_{s_2}, v_{t_1}, v_{t_2}$, say, v_{s_1}, v_{s_2}, then the associated λ should satisfy the following equation:

$$\lambda^2 - \big(1 + d_{s_1} + d_{t_1}\big)\lambda + d_{t_1}\big(1 + d_{s_1}\big) - 1 = 0. \tag{6}$$

Proof: Suppose any of situations a)–c) of Proposition 1 arises and the graph is designed from topology (f) of Fig. 1. The eigencondition is to be computed for $v_{s_1}, v_{s_2}, v_{t_1}, v_{t_2}$, respectively. First, for node v_{t_2}, since $y_k = 0$ for any $k \neq s_1, s_2, t_1, t_2$, it follows that $\sum_{i \in \mathcal{N}_{t_2 l}} y_i = 0, \sum_{i \in \mathcal{N}_{t_2 f}} y_i = y_{s_2}$. Accordingly, $d_{t_2} y_{t_2} - \sum_{i \in \mathcal{N}_{t_2}} y_i = d_{t_2} y_{t_2} - y_{s_2}$. So the eigencondition requires

$$\big(d_{t_2} - \lambda\big) y_{t_2} = y_{s_2}. \tag{7}$$

Similarly, the eigencondition of v_{t_1} requires that

$$\big(d_{t_1} - \lambda\big) y_{t_1} = y_{s_1}. \tag{8}$$

For v_{s_2}, it follows that:

$$d_{s_2} y_{s_2} - \sum_{i \in \mathcal{N}_{s_2}} y_i = d_{s_2} y_{s_2} - y_{s_1} - y_{t_2}.$$

Thus

$$\big(d_{s_2} - \lambda\big) y_{s_2} = y_{s_1} + y_{t_2}. \tag{9}$$

Similarly, the eigencondition of v_{s_1} requires

$$\big(d_{s_1} - \lambda\big) y_{s_1} = y_{s_2} + y_{t_1}. \tag{10}$$

Authorized licensed use limited to: Qingdao University. Downloaded on September 27,2020 at 09:14:25 UTC from IEEE Xplore. Restrictions apply.

This article has been accepted for inclusion in a future issue of this journal. Content is final as presented, with the exception of pagination.

Since $y_{s_1} \neq 0$ and $\bar{y}$ is an eigenvector, it can be assumed that $y_{s_1} = 1$. Consider the following circumstances.

1) Situation a) of Proposition 1 arises with a $v_k \in \mathcal{V} \setminus \{v_{s_1}, v_{s_2}, v_{t_1}, v_{t_2}\}$ incident to all $v_{s_1}, v_{s_2}, v_{t_1}, v_{t_2}$. In this situation, $y_k = 0$. Then, the eigencondition along with $\sum_{i\in\mathcal{N}_{kf}} y_i = y_{s_1} + y_{s_2} + y_{t_1} + y_{t_2}$ leads to

$$y_{s_1} + y_{s_2} + y_{t_1} + y_{t_2} = 0. \tag{11}$$

Substituting (8), (10), and $y_{s_1} = 1$ into (11) yields

$$(d_{s_1} - \lambda)(d_{t_1} - \lambda)y_{t_1} + (d_{s_1} - \lambda)^2 + (d_{s_1} - \lambda)y_{t_2} = 0. \tag{12}$$

In addition, substituting (9) and (10) into (11) and then by (7) and (8), one has

$$(d_{s_2} - \lambda)(d_{t_2} - \lambda)y_{t_2} + (d_{s_1} - \lambda)(d_{t_1} - \lambda)y_{t_1} = 0. \tag{13}$$

It can be seen from (12) and (13) that

$$y_{t_2} = \frac{(d_{s_1} - \lambda)^2}{(d_{s_2} - \lambda)(d_{t_2} - \lambda) - (d_{s_1} - \lambda)}. \tag{14}$$

Note that

$$y_{s_1} = 1. \tag{15}$$

By (8) and (7)

$$y_{t_1} = \frac{1}{(d_{t_1} - \lambda)} \tag{16}$$

$$y_{s_2} = \frac{(d_{t_2} - \lambda)(d_{s_1} - \lambda)^2}{(d_{s_2} - \lambda)(d_{t_2} - \lambda) - (d_{s_1} - \lambda)}. \tag{17}$$

Substituting (14)–(17) into (11) leads to

$$\frac{(d_{s_1} - \lambda)^2}{(d_{s_2} - \lambda)(d_{t_2} - \lambda) - (d_{s_1} - \lambda)} + \frac{1}{(d_{t_1} - \lambda)} + \frac{(d_{t_2} - \lambda)(d_{s_1} - \lambda)^2}{(d_{s_2} - \lambda)(d_{t_2} - \lambda) - (d_{s_1} - \lambda)} = -1.$$

Accordingly

$$(d_{s_1} - \lambda)^2(d_{t_2} - \lambda + 1)(d_{t_1} - \lambda) = \big[(d_{s_1} - \lambda) - (d_{s_2} - \lambda)(d_{t_2} - \lambda)\big](d_{t_1} - \lambda + 1). \tag{18}$$

Substituting (8) into (9) and (10) results in

$$(d_{s_2} - \lambda)y_{s_2} = (d_{t_1} - \lambda)y_{t_1} + y_{t_2}$$
$$(d_{s_1} - \lambda)(d_{t_1} - \lambda)y_{t_1} = y_{s_2} + y_{t_1}.$$

Then, by (7)

$$\big[(d_{s_2} - \lambda)(d_{t_2} - \lambda) - 1\big]y_{t_2} = (d_{t_1} - \lambda)y_{t_1}$$
$$\big[(d_{s_1} - \lambda)(d_{t_1} - \lambda) - 1\big]y_{t_1} = (d_{t_2} - \lambda)y_{t_2}.$$

Adding the above two equations yields

$$\big[(d_{s_2} - \lambda)(d_{t_2} - \lambda) - 1 + (d_{t_2} - \lambda)\big]y_{t_2} = \big[(d_{s_1} - \lambda)(d_{t_1} - \lambda) - 1 + (d_{t_1} - \lambda)\big]y_{t_1}. \tag{19}$$

Next, substituting (7) and (8) into (9)–(11), one has

$$\big[(d_{t_1} - \lambda) + 1\big]y_{t_1} + \big[(d_{t_2} - \lambda) + 1\big]y_{t_2} = 0$$
$$(d_{t_1} - \lambda)y_{t_1} + \big[1 - (d_{s_2} - \lambda)(d_{t_2} - \lambda)\big]y_{t_2} = 0.$$

Adding the above two equations leads to

$$\big[(d_{s_2} - \lambda)(d_{t_2} - \lambda) - 1 - (d_{t_2} - \lambda) - 1\big]y_{t_2} = \big[(d_{t_1} - \lambda) + (d_{t_1} - \lambda) + 1\big]y_{t_1}. \tag{20}$$

Let (19) minus (20), one obtains

$$\big[2(d_{t_2} - \lambda) + 1\big]y_{t_2} = \big[(d_{t_1} - \lambda)(d_{s_1} - \lambda - 1) - 2\big]y_{t_1}. \tag{21}$$

It follows from (21), (8), and $y_{s_1} = 1$ that:

$$y_{t_2} = \frac{(d_{t_1} - \lambda)(d_{s_1} - \lambda - 1) - 2}{(d_{t_1} - \lambda)[2(d_{t_2} - \lambda) + 1]}.$$

By (14)

$$(d_{s_1} - \lambda)^2(d_{t_1} - \lambda)\big[2(d_{t_2} - \lambda) + 1\big] = \big[(d_{t_1} - \lambda)(d_{s_1} - \lambda - 1) - 2\big] \times \big[(d_{s_2} - \lambda)(d_{t_2} - \lambda) - (d_{s_1} - \lambda)\big]. \tag{22}$$

From (18) and (22)

$$\frac{2(d_{t_2} - \lambda) + 1}{d_{t_2} - \lambda + 1} = \frac{(d_{t_1} - \lambda)(d_{s_1} - \lambda - 1) - 2}{d_{t_1} - \lambda + 1}.$$

Hence

$$\begin{aligned}&\big[d_{t_1}(d_{s_1} - 1) - 2\big](d_{t_2} + 1) - (2d_{t_2} + 1)(d_{t_1} + 1)\\ &\quad + \big\{(2d_{t_2} + 1) + 2(d_{t_1} + 1) - \big[d_{t_1}(d_{s_1} - 1) - 2\big]\\ &\qquad - \big[d_{t_1} + (d_{s_1} - 1)\big](d_{t_2} + 1)\big\}\lambda\\ &\quad + \big\{\big[d_{t_1} + (d_{s_1} - 1)\big] + (d_{t_2} + 1) - 2\big\}\lambda^2 - \lambda^3\\ &= 0.\end{aligned}$$

Thus, if $\bar{y}$ is an eigenvector, the corresponding eigenvalue λ should satisfy (5).

2) Situation b) arises with a $v_k \in \mathcal{V} \setminus \{v_{s_1}, v_{s_2}, v_{t_1}, v_{t_2}\}$ incident to only three of $v_{s_1}, v_{s_2}, v_{t_1}, v_{t_2}$, say $v_{s_1}, v_{s_2}, v_{t_1}$. In this situation, it follows from $\sum_{i\in\mathcal{N}_{kf}} y_i = 0$ that:

$$y_{s_1} + y_{s_2} + y_{t_1} = 0. \tag{23}$$

With $y_{s_1} = 1$, we obtain from (8) that $y_{t_1} = [1/(d_{t_1} - \lambda)]$. By (23), $y_{s_2} = -1 - [1/(d_{t_1} - \lambda)]$. It follows from (10) that:

$$(d_{s_1} - \lambda) \cdot 1 = -1 - \frac{1}{d_{t_1} - \lambda} + \frac{1}{d_{t_1} - \lambda}$$

which means $\lambda = d_{s_1} + 1$. Then, we see from (9) that

$$y_{t_2} = -1 - (d_{s_2} - d_{s_1} - 1)\left(1 + \frac{1}{d_{t_1} - d_{s_1} - 1}\right)$$

and

$$y_{t_1} = \frac{1}{d_{t_1} - d_{s_1} - 1}; \quad y_{s_2} = -1 - \frac{1}{d_{t_1} - d_{s_1} - 1}.$$

3) Situation c) arises with a $v_k \in \mathcal{V} \setminus \{v_{s_1}, v_{s_2}, v_{t_1}, v_{t_2}\}$ incident to only two of $v_{s_1}, v_{s_2}, v_{t_1}, v_{t_2}$, say v_{s_1}, v_{s_2}. Similar

Authorized licensed use limited to: Qingdao University. Downloaded on September 27,2020 at 09:14:25 UTC from IEEE Xplore. Restrictions apply.

This article has been accepted for inclusion in a future issue of this journal. Content is final as presented, with the exception of pagination.

arguments as (23) yields $y_{s_1} + y_{s_2} = 0$. Since $y_{s_1} = 1$ and $y_{s_2} = -1$. By (9) and (10)

$$y_{t_2} = -1 - \big(d_{s_2} - \lambda\big), y_{t_1} = 1 + \big(d_{s_1} - \lambda\big).$$

By (8), $(d_{t_1} - \lambda)[1 + (d_{s_1} - \lambda)] = 1$, that is, (6) holds. ■

Proposition 2: For graphs designed from (f) of Fig. 1, the expected QCD topology structures are (b), (c), (f), and (i) of Fig. 2; (b) and (e) of Fig. 4; (f) of Fig. 5; (e) of Fig. 6; (d) of Fig. 7; (c) of Fig. 8; (b) and (e) of Fig. 9; and (a) of Fig. 10; and v_3, v_4, v_5, and v_6 in these graphs are the corresponding QCD nodes.

Proof: The result can be obtained by applying Lemma 1 directly to Figs. 2–10. ■

For graphs designed from other topologies of Fig. 1, the QCD topology structures can be achieved in the same way.

Lemma 2 [48]: The multiagent system with dynamics (1) is controllable if and only if there is no eigenvector of $\mathcal{G}$ taking 0 on the elements corresponding to the leaders.

Theorem 1: If the multiagent system is controllable, then the interconnection graph does not have the identified topology structures of QCD nodes in Proposition 2.

Proof: For the graph (b) of Fig. 2, the QCD nodes are v_3, v_4, v_5, and v_6; and $d_1 = 1, d_2 = 5, d_3 = d_5 = 3, d_4 = d_6 = 2$. The eigencondition associated with v_1 requires $d_1 y_1 - y_2 = \lambda y_1$, which can be met if we set $y_1 = y_2 = 0$. For v_2, the eigencondition yields $5y_2 - (y_1 + y_3 + y_4 + y_5 + y_6) = \lambda y_2$. With $y_1 = y_2 = 0$, one has $y_3 + y_4 + y_5 + y_6 = 0$. For v_3, v_4, v_5, and v_6, the eigencondition, respectively, yields the following equations:

$$\begin{aligned} d_3 y_3 - (y_2 + y_5 + y_6) &= \lambda y_3 \\ d_4 y_4 - (y_2 + y_5) &= \lambda y_4 \\ d_5 y_5 - (y_2 + y_3 + y_4) &= \lambda y_5 \\ d_6 y_6 - (y_2 + y_3) &= \lambda y_6. \end{aligned}$$

With $y_1 = y_2 = 0$, and substituting $d_i, i = 3, 4, 5, 6$ into the above equations, one has $(3 - \lambda)y_3 = y_5 + y_6$; $(2 - \lambda)y_4 = y_5$; $(3 - \lambda)y_5 = y_3 + y_4$; and $(2 - \lambda)y_6 = y_3$. Set $y_3 = y_5 = 1$, and note that $\lambda = 3$ is an eigenvalue, it follows from the above equations that $\bar{y} = [0, 0, 1, -1, 1, -1]^T$ is an eigenvector of the graph (b) of Fig. 2, as can be verified directly. It can be shown in the same way that for the other QCD topologies, the corresponding Laplacian $\mathcal{L}$ has an eigenvector in the form of $\bar{y}$. By Lemma 2, the system is uncontrollable with the first and second agent taking leaders role. This contradicts the fact that the system is controllable. The proof is completed. ■

Remark 1: The above analysis demonstrates an identification process for controllability destructive nodes of any graph. Although the process only involves the QCD case, it applies to the discovery of other destructive nodes. For example, the identification of quintuple controllability destructive (QuinCD) nodes in the next section, which, however, does not need to be considered in a five-node graph. With each increase in the number of nodes, a new class of destructive topology to be identified appears. Although the identification method is the same, the specific implementation varies greatly, which brings much difficulty to the problem. Theorem 2 is another necessary condition, which is pertinent to the topologies of QuinCD nodes. By applying the same treatments as Theorems 1 and 2 to other situations, more destructive topologies can be found out. When all the destructive nodes are identified, the complete graphic characterization of controllability is achieved. Thus, a graph-theory-based sufficient and necessary condition can be obtained for any leader selection.

4) Complexity and Design Procedure: The above design process is summarized as follows.

Step 1: Divide the nodes of the graph into two groups, say, the above $\{v_1, v_2\}$ and $\{v_3, v_4, v_5, v_6\}$.

Step 2: Depict the topology structures formed by these two groups of nodes, respectively, say, the above Figs. 1 and Ξ.

Step 3: Design candidate QCD nodes by taking advantage of Proposition 1.

Step 4: Identify the QCD nodes from the candidate topologies by using, say, Lemma 1.

Although the idea of the design process is universal, the graphic controllability characterization for graphs with different number of nodes is ever-changing. So each graph with a fixed number of nodes has its own research value, even if the number difference of nodes is just 1. That is why we illustrate the process with graphs of six nodes, whose specific topology features cannot be replaced by graphs with four or five nodes.

Remark 2: The complexity is reviewed as follows.

1) The complexity of characterizing graphic controllability stems from step 2. The specific reasons are as follows. For a graph consisting of n nodes, each subgraph in Ξ consists of $n - 4$ nodes because we are considering the design of QCD nodes. Thus, corresponding to the graph composed of five nodes, there is only one subgraph in Ξ, which consists of a single node. However, for a graph of six nodes, the subgraph in Ξ becomes two. This not only doubles the number of diagrams to be described in Ξ but also at least doubles the number of diagrams to be designed and identified in steps 3 and 4. Let us make another comparison between the graphs of seven and eight nodes. For the graph consisting of seven nodes, the number of topology structures in Ξ is 4; while for the graph of eight nodes, the number is 11. In general, the number of topologies in Ξ increases by $\sum_{i=1}^{n-4} C_{n-4}^{i} = 2^{n-4} - 1$ for each additional node that makes up the graph. So the aforementioned complexity has more than tripled even though the number of nodes has only increased by one. The above analysis implies that the addition of only one node at least doubles the complexity of steps 2–4. This is just the complexity of adding one node in the interconnection graph, let alone more. Therefore, the complexity caused by the increase in the number of nodes increases geometrically.
2) More seriously, this increasing trend in complexity also exists in the design and identification of each of the other controllability destructive nodes, say, QuinCD nodes in the next section. With the increase of the number of nodes, new destructive topologies have emerged for

Authorized licensed use limited to: Qingdao University. Downloaded on September 27,2020 at 09:14:25 UTC from IEEE Xplore. Restrictions apply.

This article has been accepted for inclusion in a future issue of this journal. Content is final as presented, with the exception of pagination.

investigation. For example, QinCD nodes in six-node graphs would not appear in a five-node graph for study.

3) Even for the same kind of controllability destructive topology, the specific form and quantity of this kind of topology are very different in the graph composed by different number of nodes. For example, the specific content and form of Proposition 1 and Lemma 1 vary with the number of nodes in a graph. The results of this article on a graph of six nodes and that paper [18] on five nodes illustrate and compare this well.
4) Although the previous steps and processes apply to all graphs, each graph composed of different number of nodes has its own independent research value because each type of graph has very different forms and numbers of destructive topology structures. The above discussion also shows that the complete graphic characterization of the controllability of any given graph with a fixed number of nodes cannot replace that of any other graphs with different node numbers. This is a major feature of complete graphic controllability characterization, as opposed to establishing results for only one type of selected leaders.

B. Quintuple Destructive Nodes

Even with early filtering, this section will show in detail that all the quintuple destructive nodes still need to be identified from the 1364 candidate topology structures.

1) Result for Topologies Design: For graphs of six vertices, to investigate QuinCD nodes, we consider an eigenvector $\bar{y} = [0, y_2, y_3, y_4, y_5, y_6]^T$, $y_2, y_3, y_4, y_5, y_6 \neq 0$. Each entry of $\bar{y}$ satisfies the eigencondition. Below, without loss of generality, v_1 is taken as the leader. For v_1, its $\mathcal{N}_{1f}$ has the following cases:

1) $2, 3, 4, 5, 6 \in \mathcal{N}_{1f}$. In this case, v_2, v_3, v_4, v_5, v_6 are the neighbor nodes of v_1;
2) any four and only four of $2, 3, 4, 5, 6$ belong to $\mathcal{N}_{1f}$;
3) any three and only three of $2, 3, 4, 5, 6$ belong to $\mathcal{N}_{1f}$;
4) any two and only two of $2, 3, 4, 5, 6$ belong to $\mathcal{N}_{1f}$;
5) any one and only one of $2, 3, 4, 5, 6$ belongs to $\mathcal{N}_{1f}$;
6) none of $2, 3, 4, 5, 6$ belong to $\mathcal{N}_{1f}$.

Proposition 3: For a graph $\mathcal{G}$ consisting of six vertices, if v_1 is selected, without loss of generality, as the single leader, then the following statements hold:

1) case 6) does not happen;
2) the index k of any single node v_k cannot be associated with two different cases at the same time;
3) any two cases cannot occur simultaneously;
4) for any given case, this case cannot occur on two different sets of nodes.

Proof: For node v_1, since $y_1 = 0$, it follows that:

$$d_1 y_1 - \sum_{i \in \mathcal{N}_1} y_i = -\sum_{i \in \mathcal{N}_{1f}} y_i. \tag{24}$$

Combining the eigencondition with (24) yields

$$\sum_{i \in \mathcal{N}_{1f}} y_i = 0. \tag{25}$$

First, case 6) does not happen because of the connectedness of the graph. On case 1), since $\sum_{i \in \mathcal{N}_{1f}} y_i = y_2 + y_3 + y_4 + y_5 + y_6$, by (25)

$$y_2 + y_3 + y_4 + y_5 + y_6 = 0. \tag{26}$$

On case 2), suppose, no loss of generality, that $2, 3, 4, 5 \in \mathcal{N}_{1f}$, then $\sum_{i \in \mathcal{N}_{1f}} y_i = y_2 + y_3 + y_4 + y_5$. By (25)

$$y_2 + y_3 + y_4 + y_5 = 0. \tag{27}$$

Equations (26) and (27) cannot be met simultaneously, or else, $y_6 = 0$. This is in contradiction with the prerequisite condition $y_6 \neq 0$. Thus, cases 1) and 2) cannot be met simultaneously. In general, since the graph is simple, there are no repeated edges between any two nodes. Accordingly, if v_k is a neighbor of v_1 and the index k is associated with a certain case, say case 2), then v_k cannot be associated with another case, say case 3). That is to say, the index k of any single node v_k cannot be associated with two different cases at the same time because the leader is single. A direct consequence of this observation is that if case 1) happens, no other case can happen.

Case 2) happens on one and only one node set consisting of the four nodes from v_2, v_3, v_4, v_5, v_6. Otherwise, case 1) will occur. For example, the following two situations $2, 3, 4, 5 \in \mathcal{N}_{1f}$ and $3, 4, 5, 6 \in \mathcal{N}_{1f}$ cannot happen simultaneously, because these two cases share at least one common node, say v_3. If the two cases occur simultaneously, there is a repeated edge between v_1 and v_3; and case 1) occurs, as is a contradiction. Also, cases 2) and 5) cannot happen at the same time, otherwise case 1) occurs. So, if case 2) happens, no other case can happen.

Since the leader is single and there are no repeated edges between any two nodes, similar arguments as cases 1) and 2) show that the following two facts hold: any two cases cannot occur simultaneously; and for any given case, this case cannot occur on two different sets of nodes. For example, if case 5) occurs, respectively, on nodes v_2 and v_3, then case 4) happens. Thus, case 5) cannot happen simultaneously on two different sets of nodes. ■

2) Design of Candidate Topologies: To build graphs by Proposition 3, we first consider topologies consisting of all five follower nodes v_2–v_6. They form a total of 44 different topologies. The following two figures show only 22 of them, and the others are not listed for space limitation.

Let us take, for example, (b) of Fig. 12 to illustrate the design of candidate topologies. The same process applies to other diagrams in Figs. 11 and 12. Combining leader v_1 with (b) of Fig. 12 yields (a) of Fig. 13, which is the original graph for construction. The construction is based on the

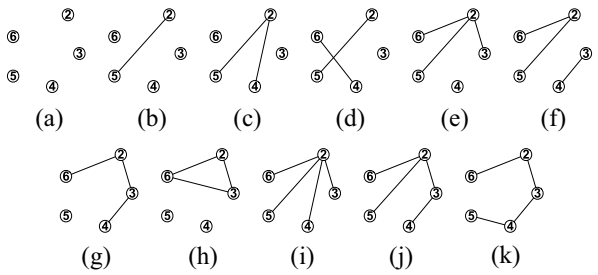

Fig. 11. Group of topologies consisting of v_2, v_3, v_4, v_5, and v_6.

Authorized licensed use limited to: Qingdao University. Downloaded on September 27,2020 at 09:14:25 UTC from IEEE Xplore. Restrictions apply.

This article has been accepted for inclusion in a future issue of this journal. Content is final as presented, with the exception of pagination.

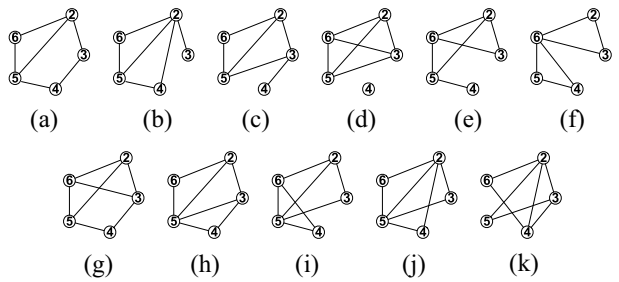

Fig. 12. Another group of topologies consisting of v_2, v_3, v_4, v_5, and v_6.

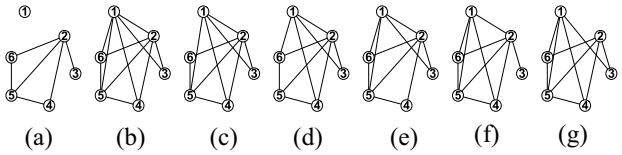

Fig. 13. (a) is the original graph for construction; graph (b) is designed by case 1); and graphs (c)–(g) are designed by case 2).

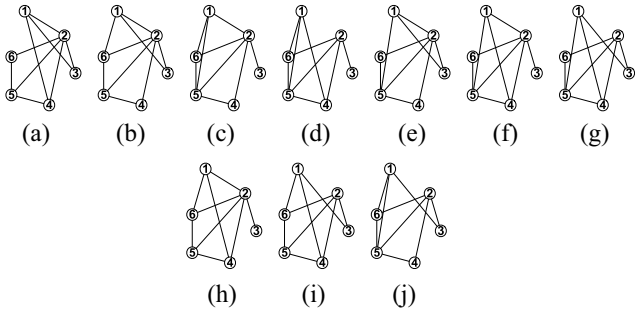

Fig. 14. Graphs (a)–(j) are designed by case 3).

information flow designed between $\{v_1\}$ and $\{v_2, v_3, v_4, v_5, v_6\}$ by using Proposition 3. For cases 1)–6) mentioned just before Proposition 3, Proposition 3 tells us that we need to consider the following circumstances to design the candidate QuinCD nodes.

1) *Case 1) Occurs:* In this case, graph (b) of Fig. 13 is designed.
2) *Case 2) Occurs:* In this case, graphs (c)–(g) of Fig. 13 are designed by Proposition 3.
3) *Case 3) Occurs:* In this case, graphs (a)–(j) of Fig. 14 are designed by Proposition 3.
4) *Case 4) Occurs:* In this case, graphs (a)–(j) of Fig. 15 are designed by Proposition 3.
5) *Case 5) Occurs:* In this case, graphs (a)–(e) of Fig. 16 are designed by Proposition 3.

3) Identification:

Lemma 3: Suppose $\bar{y} = [0, y_2, y_3, y_4, y_5, y_6]^T$ is an eigenvector of a graph designed from (b) of Fig. 12, where $y_2, y_3, y_4, y_5, y_6 \neq 0$. Then, $y_i's$ take the following values:

$$y_2 = k, \text{ where } k \text{ is an arbitrary nonzero real number given in advance}$$

$$y_3 = -\frac{1}{d_3 - \lambda}k$$

$$y_4 = k + \left\{[(d_2 - \lambda) + 1] + \frac{1}{d_3 - \lambda}\right\}\frac{k}{(d_4 - \lambda)[1 + (d_5 - \lambda)]}$$

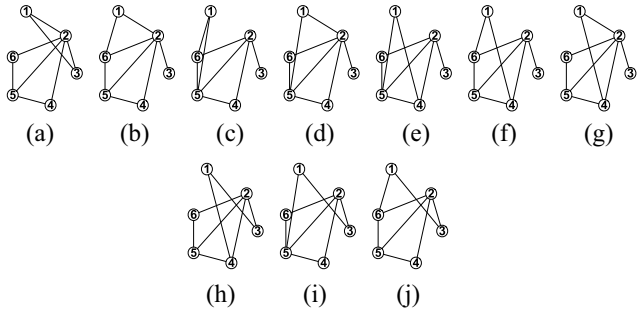

Fig. 15. Graphs (a)–(j) are designed by case 4).

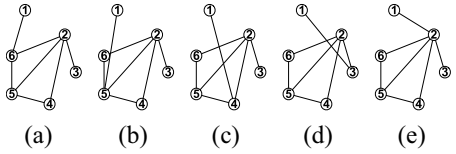

Fig. 16. Graphs (a)–(e) are designed by case 5).

$$y_5 = \left\{[(d_2 - \lambda) + 1] + \frac{1}{d_3 - \lambda}\right\}\frac{1}{1 + (d_5 - \lambda)}k$$

$$y_6 = \frac{k}{(d_6 - \lambda)[1 + (d_5 - \lambda)]} \times \left\{(d_4 - \lambda)[1 + (d_5 - \lambda)] + [(d_2 - \lambda) + 1] + \frac{1}{d_3 - \lambda}\right\}.$$

Proof: First, suppose any of the cases 1)–5) happens and the graph is designed from (b) of Fig. 12. Let eigenvalue λ correspond to the eigenvector $\bar{y}$. We verify the eigencondition for each of $y_i's$, $i = 2, 3, 4, 5, 6$. For node v_2, since $y_1 = 0$ and v_1 is the leader, we see that $\sum_{i\in\mathcal{N}_{2l}} y_i = 0$ and $\sum_{i\in\mathcal{N}_{2f}} y_i = y_3 + y_4 + y_5 + y_6$. Then

$$\sum_{i\in\mathcal{N}_2} y_i = \sum_{i\in\mathcal{N}_{2l}} y_i + \sum_{i\in\mathcal{N}_{2f}} y_i = y_3 + y_4 + y_5 + y_6.$$

Since the eigencondition requires

$$d_2 y_2 - \sum_{i\in\mathcal{N}_2} y_i = \lambda y_2$$

for node v_2, the following condition should be satisfied:

$$(d_2 - \lambda)y_2 = (y_3 + y_4 + y_5 + y_6). \tag{28}$$

Applying the same procedure to vertices v_3, v_4, v_5, and v_6, respectively, produces the following conditions (29)–(32) that should be satisfied. For v_3

$$d_3 y_3 - \sum_{i\in\mathcal{N}_3} y_i = d_3 y_3 - \sum_{i\in\mathcal{N}_{3f}} y_i = d_3 y_3 - y_2 = \lambda y_3$$

which yields

$$(d_3 - \lambda)y_3 = -y_2. \tag{29}$$

For v_4

$$d_4 y_4 - \sum_{i\in\mathcal{N}_4} y_i = d_4 y_4 - \sum_{i\in\mathcal{N}_{4f}} y_i$$

Authorized licensed use limited to: Qingdao University. Downloaded on September 27,2020 at 09:14:25 UTC from IEEE Xplore. Restrictions apply.

This article has been accepted for inclusion in a future issue of this journal. Content is final as presented, with the exception of pagination.

$$= d_4 y_4 - (y_2 + y_5)$$
$$= \lambda y_4$$

which yields

$$(d_4 - \lambda) y_4 = y_2 + y_5. \tag{30}$$

For v_5

$$d_5 y_5 - (y_2 + y_4 + y_6) = \lambda y_5$$

which means

$$(d_5 - \lambda) y_5 = y_2 + y_4 + y_6. \tag{31}$$

For v_6

$$(d_6 - \lambda) y_6 = y_2 + y_5. \tag{32}$$

Substituting (29) into (28) and (30)–(32), respectively, produces the following equations to be satisfied:

$$[-(d_2 - \lambda)(d_3 - \lambda) - 1] y_3 = y_4 + y_5 + y_6 \tag{33}$$
$$(d_4 - \lambda) y_4 + (d_3 - \lambda) y_3 = y_5 \tag{34}$$
$$(d_5 - \lambda) y_5 + (d_3 - \lambda) y_3 = y_4 + y_6 \tag{35}$$
$$(d_6 - \lambda) y_6 + (d_3 - \lambda) y_3 = y_5. \tag{36}$$

By (34) and (36)

$$(d_6 - \lambda) y_6 = (d_4 - \lambda) y_4. \tag{37}$$

By (33) and (35)

$$\{[-(d_2 - \lambda) - 1](d_3 - \lambda) - 1\} y_3 = [1 + (d_5 - \lambda)] y_5. \tag{38}$$

Since $y_2 \neq 0$ and $\bar{y}$ is an eigenvector, we can assume that $y_2 = 1$. It follows from (29) and (38) that:

$$y_3 = -\frac{1}{d_3 - \lambda}$$
$$y_5 = \left\{[(d_2 - \lambda) + 1] + \frac{1}{d_3 - \lambda}\right\} \frac{1}{1 + (d_5 - \lambda)}.$$

Moreover, we obtain from (34) and (37) that

$$y_4 = 1 + \left\{[(d_2 - \lambda) + 1] + \frac{1}{d_3 - \lambda}\right\} \frac{1}{(d_4 - \lambda)[1 + (d_5 - \lambda)]}$$
$$y_6 = \frac{1}{(d_6 - \lambda)[1 + (d_5 - \lambda)]} \times \left\{(d_4 - \lambda)[1 + (d_5 - \lambda)] + [(d_2 - \lambda) + 1] + \frac{1}{d_3 - \lambda}\right\}$$

This completes the proof. ■

Lemma 3 enables us to identify the QuinCD structures, which are (b), (d), (f), and (g) of Fig. 13; (d), (e), (h), and (i) of Fig. 14; (a), (d), (f), and (i) of Fig. 15; and (b), (d), and (e) of Fig. 16. So v_2, v_3, v_4, v_5, and v_6 in these graphs are the corresponding QuinCD nodes.

Theorem 2: If the multiagent system is controllable, then the graph does not have the above-identified topology structures of QuinCD nodes. In addition, 3432 is the maximum number of candidate graphs to identify all destructive nodes.

Proof: The first part of the result can be proved in the same vein as Theorem 1. For the second part, let us start with QCD nodes. There are a total of 94 topologies from Figs. 2–10 which, by Definition 2, are said to be designed from (f) of Fig. 1 except for the original graph (a) of Fig. 2. Corresponding to the graph (f) of Fig. 1, these 94 candidate topologies are to be identified to find QCD nodes. Because (f) of Fig. 1 and (b) of Ξ are, respectively, just one diagram in Fig. 1 and Ξ, the total number of topologies to be identified is $94 \times 11 \times 2 = 2068$.

Next, we consider QuinCD nodes. Corresponding to (b) of Fig. 12, there are 31 designed candidate graphs from Figs. 13–16 to be identified for QuinCD nodes. The graph (a) of Fig. 13 is the original diagram which is not in the 31 candidate graphs. Since Figs. 11 and 12 have 44 diagrams, there will be a total of $31 \times 44 = 1364$ designed candidate graphs that will be used to identify all the QuinCD nodes. The second part then follows from the above arguments. ■

Remark 3: A sufficient and necessary condition is achieved when all the necessary conditions as Theorems 1 and 2 come together, which is exactly the complete graphic characterization of controllability. This workload is huge, unlike the five-node graph that can be given in one article. Compared to the number 6944 mentioned in Section I, 3432 is a significantly reduced result.

IV. Essentially Controllable Graphs

The concept of essential controllability was put forward by Aguilar and Gharesifard [1]. The associated graphs do not contain any destructive nodes, which constitute a class of interesting topologies to be found in the characterization.

Definition 3 [1]: A system is said to be essentially controllable if it is controllable under any leaders selection. Here, both the number and the locations of leaders are arbitrary.

Theorem 3: A system is essentially controllable if and only if all the eigenvalues of Laplacian $\mathcal{L}$ of the graph are distinct and each eigenvector has no zero elements.

Proof (Necessity): Suppose by contradiction that there is an eigenvalue λ of $\mathcal{L}$ with its algebraic multiplicity n_λ greater than 1, that is, $n_\lambda > 1$. Since the graph is undirected, $\mathcal{L}$ is symmetric and accordingly there are n_λ linearly independent eigenvectors of λ. Let η_1 and η_2 be any two eigenvectors of λ. There is a linear combination $\eta = \alpha_1 \eta_1 + \alpha_2 \eta_2$ of η_1 and η_2 so that η has at least one zero element, where α_1 and α_2 are real numbers. Note that η is also an eigenvector of λ since so is for both η_1 and η_2. Then, by Lemma 2, the system is uncontrollable if leaders are selected from the agents corresponding to the zero elements of η, which is a contradiction to the essential controllability. The above discussion also yields that any eigenvector of $\mathcal{L}$ has no zero elements because the system is essentially controllable.

Sufficiency: Since each eigenvalue of $\mathcal{L}$ is different from all the others, and the eigenvector of each eigenvalue has no zero elements, the system is controllable with any selection of leaders. Otherwise, by Lemma 2, the uncontrollability of the system under a group of leaders implies that $\mathcal{L}$ has an eigenvector with the elements corresponding to the leader agents taking the value of zero. This is a contradiction to the assumption. ■

Authorized licensed use limited to: Qingdao University. Downloaded on September 27,2020 at 09:14:25 UTC from IEEE Xplore. Restrictions apply.

This article has been accepted for inclusion in a future issue of this journal. Content is final as presented, with the exception of pagination.

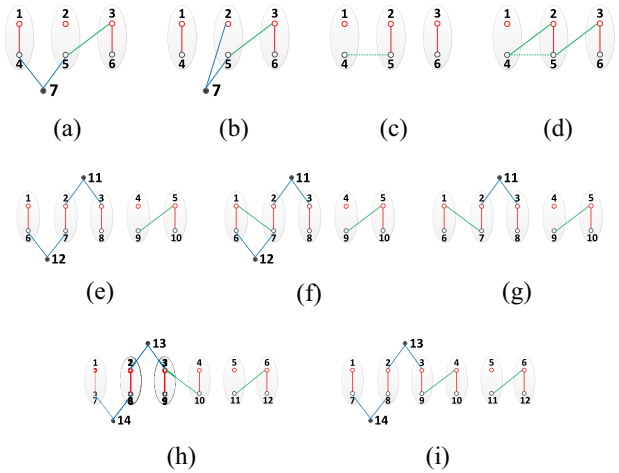

Fig. 17. (a)–(i) are the topology structures.

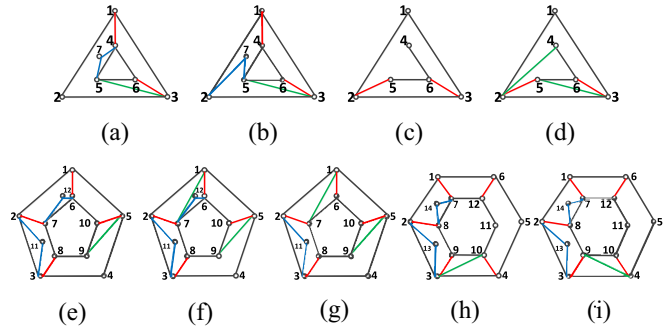

Fig. 18. (a)–(i) are the topology structures corresponding to, respectively, each of the figures in Fig. 17.

Fig. 19. All undirected connected graphs of three nodes.

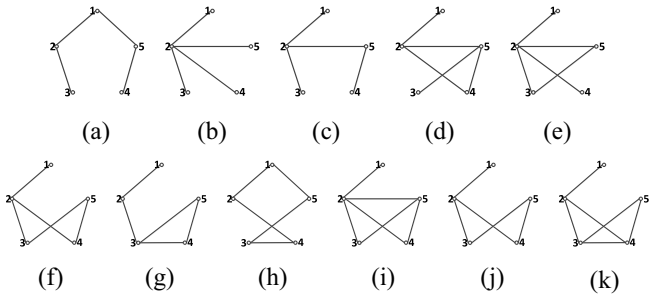

Fig. 20. Part one of all connected graphs of five nodes.

The next goal is to cast the algebraic condition of Theorem 3 on the meaning of topology structures by finding topology graphs satisfying the condition. The ideas for the design procedure proposed in [57] are listed as follows:

1) divide the nodes into two groups Ω_1 and Ω_2;
2) set double nodes sets with each node belonging to one and only one double node set;
3) depict the corresponding schematic and the associated original graph; say (a) and (b) of Fig. 1 of [57];
4) focus on the two unfixed double nodes sets and design the associated essentially controllable graphs. Refer to [57, steps 2–6] for detailed implementation;
5) start from the two fixed double nodes sets and design the essentially controllable graphs. Refer to [57, step 7] for detailed implementation.

The schematic and the fixed and unfixed double nodes sets are two main features of the proposed design method. The verification in [57] shows that many essentially controllable graphs can be constructed by the above method, as is shown in subsequent arguments.

Theorem 4: The system is essentially controllable with each of the following designed graphs: (a), (b), and (d)–(f) of Fig. 6; (a)–(c) of Fig. 8; (a), (b), (d)–(h), (k), and (l) of Fig. 10; (a)–(d) of Fig. 12; and all the graphs in Fig. 14 except the one (j), where all the figures mentioned here refer to those of [57].

Below, more essentially controllable graphs that are not discovered in [57] are constructed using the above method.

Four essentially controllable graphs are produced when the design steps are applied to a situation of six nodes. More specifically, as done in [57, step 1], the six nodes are divided into two groups $\Omega_1 = \{1, 2, 3\}$ and $\Omega_2 = \{4, 5, 6\}$. Then, the construction steps 2–4 of [57] produce the diagrams (a) and (b) of Fig. 17. The corresponding topology graphs are, respectively, (a) and (b) of Fig. 18, which are verified to be essentially controllable. By the case a) of step 4 of [57], we obtain diagrams (c) and (d) of Fig. 17, where the dotted edge between nodes 4 and 5 means that the edge e_{45} is removed in the construction. The corresponding topology graphs are, respectively, (c) and (d) of Fig. 18, which are also essentially controllable.

If the construction steps are applied to a situation of ten nodes, there are going to be more graphs produced than there are scenarios starting at eight nodes. Here, we only list the three resulting diagrams (e)–(g) of Fig. 17 and the corresponding topology graphs (e)–(g) of Fig. 18, which are verified to be essentially controllable.

Similarly, diagrams (h) and (i) are constructed from 12 nodes, and the corresponding topology graphs (h) and (i) of Fig. 18 are also essentially controllable.

Theorem 5: If the number of nodes forming a graph is not less than 3, then the minimum number of nodes for an essentially controllable graph is 6.

Proof: The result is verified by, respectively, considering the graphs consisting of three nodes, four nodes, and five nodes.

All the undirected connected graphs of three nodes, four nodes, and five nodes are, respectively, depicted in Fig. 19; (a)–(d), (f), and (h) of Figs. 1, 20, and 21. It can be verified, by calculation, that there is not any essentially controllable graph. Since one of the essentially controllable graphs of six nodes is shown in (c) or (d) of Fig. 18, the conclusion is valid. ■

Authorized licensed use limited to: Qingdao University. Downloaded on September 27,2020 at 09:14:25 UTC from IEEE Xplore. Restrictions apply.

This article has been accepted for inclusion in a future issue of this journal. Content is final as presented, with the exception of pagination.

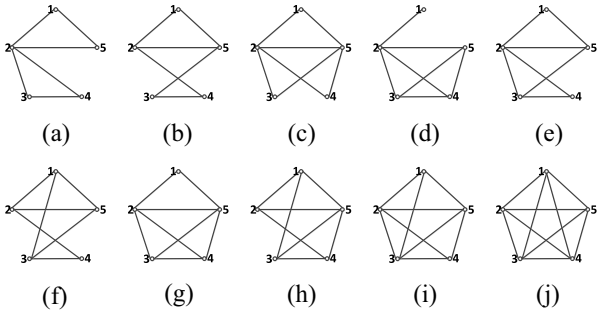

Fig. 21. Part two of all connected graphs of five nodes.

V. Conclusion

This article analyzed how leaders selection leads to the complexity on graph-theoretic characterizations of controllability. Through the general steps proposed, the topology structures of information flow between leaders and followers were constructively designed and identified, which provided a way for us to quantitatively evaluate the complexity of the graph-theoretic characterization. Based on this, we can see how the complexity at least doubles even if the number of nodes that make up the graph increases by only one. As a byproduct, it can be seen that although the proposed design and identification process is applicable in all cases, the controllability characterization of graphs composed of different number of nodes is kaleidoscopic and the controllability of each kind of graphs with a different number of nodes has completely different specific characteristics.

The design and identification process was illustrated by a detailed analysis of six-node graphs, which indicated that up to 3432 destructive topologies need to be eliminated from the 6944 topological diagrams to obtain the complete graphic characterization. As with most results established previously in the field, which were derived only for a class or classes of leaders, the above efforts implied that even if there was a result that is both sufficient and necessary, it is far from answering the complete controllability graphic characterization for any leader selection. Our analysis also indicated, to some extent, that the complexity of uncovering controllability graphic characterizations is usually much higher than that of establishing algebraic conditions. This is why the seemingly simple algebraic conditions are so involved to explain on a graph-theoretic level.

As a supplement to the complete graphic characterization of controllability, the essentially controllable graph has also been studied, which are the controllable graphs no matter how the leader nodes are selected. A necessary and sufficient condition was given for the essential controllability. Starting from a simple topology structure, lots of essentially controllable graphs were constructed by following the proposed design procedure.

References

[1] C. O. Aguilar and B. Gharesifard, "Graph controllability classes for the Laplacian leader–follower dynamics," *IEEE Trans. Autom. Control*, vol. 60, no. 6, pp. 1611–1623, Jun. 2015.

[2] G. Notarstefano and G. Parlangeli, "Controllability and observability of grid graphs via reduction and symmetries," *IEEE Trans. Autom. Control*, vol. 58, no. 7, pp. 1719–1731, Jul. 2013.

[3] G. Parlangeli and G. Notarstefano, "On the reachability and observability of path and cycle graphs," *IEEE Trans. Autom. Control*, vol. 57, no. 3, pp. 743–748, Mar. 2012.

[4] C. Sun, G. Hu, and L. Xie, "Controllability of multi-agent networks with antagonistic interactions," *IEEE Trans. Autom. Control*, vol. 62, no. 10, pp. 5457–5462, Oct. 2017.

[5] Y. Guan, Z. Ji, L. Zhang, and L. Wang, "Controllability of heterogeneous multi-agent systems under directed and weighted topology," *Int. J. Control*, vol. 89, no. 5, pp. 1009–1024, 2016.

[6] R. Lozano, M. W. Spong, J. A. Guerrero, and N. Chopra, "Controllability and observability of leader-based multi-agent systems," in *Proc. 47th IEEE Conf. Decis. Control*, Dec. 2008, pp. 3713–3718.

[7] Z. Ji, H. Lin, and H. Yu, "Leaders in multi-agent controllability under consensus algorithm and tree topology," *Syst. Control Lett.*, vol. 61, no. 9, pp. 918–925, Jul. 2012.

[8] A. Rahmani, M. Ji, M. Mesbahi, and M. Egerstedt, "Controllability of multi-agent systems from a graph-theoretic perspective," *SIAM J. Control Optim.*, vol. 48, no. 1, pp. 162–186, 2009.

[9] M. Nabi-Abdolyousefi and M. Mesbahi, "On the controllability properties of circulant networks," *IEEE Trans. Autom. Control*, vol. 58, no. 12, pp. 3179–3184, Apr. 2013.

[10] M. Egerstedt, S. Martini, M. Cao, K. Camlibel, and A. Bicchi, "Interacting with networks: How does structure relate to controllability in single-leader, consensus networks?" *IEEE Control Syst. Mag.*, vol. 32, no. 4, pp. 66–73, Jul. 2012.

[11] B. She, S. Mehta, C. Ton, and Z. Kan, "Controllability ensured leader group selection on signed multiagent networks," *IEEE Trans. Cybern.*, vol. 50, no. 1, pp. 222–232, Jan. 2020, doi: 10.1109/TCYB.2018.2868470.

[12] X. Liu, Z. Ji, and T. Hou, "Graph partitions and the controllability of directed signed networks," *Sci. China Inf. Sci.*, vol. 62, Apr. 2019, Art. no. 42202, doi: 10.1007/s11432-018-9450-8.

[13] T. Zhou, "On the controllability and observability of networked dynamic systems," *Automatica*, vol. 52, pp. 63–75, Feb. 2015.

[14] N. Cai, M. He, Q. Wu, and M. J. Khan, "On almost controllability of dynamical complex networks with noises," *J. Syst. Sci. Complexity*, vol. 32, no. 4, pp. 1125–1139, 2019, doi: 10.1007/s11424-017-6273-7.

[15] M. Cao, S. Zhang, and M. K. Camlibel, "A class of uncontrollable diffusively coupled multi-agent systems with multi-chain topologies," *IEEE Trans. Autom. Control*, vol. 58, no. 2, pp. 465–469, Feb. 2013.

[16] Y. Guan, Z. Ji, L. Zhang, and L. Wang, "Decentralized stabilizability of multi-agent systems under fixed and switching topologies," *Syst. Control Lett.*, vol. 62, no. 5, pp. 438–446, 2013.

[17] B. Zhao, Y. Guan, and L. Wang, "Controllability improvement for multi-agent systems: Leader selection and weight adjustment," *Int. J. Control*, vol. 89, no. 10, pp. 2008–2018, 2016.

[18] Z. Ji and H. Yu, "A new perspective to graphical characterization of multi-agent controllability," *IEEE Trans. Cybern.*, vol. 47, no. 6, pp. 1471–1483, Jun. 2017.

[19] Y. Zheng, J. Ma, and L. Wang, "Consensus of hybrid multi-agent systems," *IEEE Trans. Neural Netw. Learn. Syst.*, vol. 29, no. 4, pp. 1359–1365, Apr. 2018.

[20] H. Su, H. Wu, and J. Lam, "Positive edge-consensus for nodal networks via output feedback," *IEEE Trans. Autom. Control*, vol. 64, no. 3, pp. 1244–1249, Mar. 2019.

[21] Y. Gao, B. Liu, J. Yu, J. Ma, and T. Jiang, "Consensus of first-order multi-agent systems with intermittent interaction," *Neurocomputing*, vol. 129, pp. 273–278, Apr. 2014.

[22] J. Qu, Z. Ji, C. Lin, and H. Yu, "Fast consensus seeking on networks with antagonistic interactions," *Complexity*, vol. 2018, Dec. 2018, Art. no. 7831317. [Online]. Available: https://doi.org/10.1155/2018/7831317

[23] L. Pan, H. Shao, M. Mesbahi, Y. Xi, and D. Li, "Bipartite consensus on matrix-valued weighted networks," *IEEE Trans. Circuits Syst. II, Exp. Briefs*, vol. 66, no. 8, pp. 1441–1445, Aug. 2019.

[24] Z. Gan, H. Shao, and Y. Xu, "Performance of leader-following consensus on multiplex networks," *Physica A Stat. Mech. Appl.*, vol. 509, pp. 1174–1182, Nov. 2018.

[25] S. S. Alaviani and N. Elia, "Distributed multi-agent convex optimization over random digraphs," *IEEE Trans. Autom. Control*, early access, doi: 10.1109/TAC.2019.2937499.

[26] L. Zhang, Z. Ning, and Z. Wang, "Distributed filtering for fuzzy time-delay systems with packet dropouts and redundant channels," *IEEE Trans. Syst., Man, Cybern., Syst.*, vol. 46, no. 4, pp. 559–572, Apr. 2015.

Authorized licensed use limited to: Qingdao University. Downloaded on September 27,2020 at 09:14:25 UTC from IEEE Xplore. Restrictions apply.

This article has been accepted for inclusion in a future issue of this journal. Content is final as presented, with the exception of pagination.

[27] X. Yin, J. Zeng, and J. Liu, "Forming distributed state estimation network from decentralized estimators," *IEEE Trans. Control Syst. Technol.*, vol. 27, no. 6, pp. 2430–2443, Nov. 2019.
[28] X. Yin, L. Zhang, Z. Ning, D. Tian, A. Alsaedi, and B. Ahmad, "State estimation via Markov switching-channel network and application to suspension systems," *IET Control Theory Appl.*, vol. 11, no. 3, pp. 411–419, Jan. 2017.
[29] F. Xiao, Y. Shi, and W. Ren, "Robustness analysis of asynchronous sampled-data multi-agent networks with time-varying delays," *IEEE Trans. Autom. Control*, vol. 63, no. 7, pp. 2145–2152, Jul. 2018.
[30] F. Xiao, T. Chen, and H. Gao, "Synchronous hybrid event- and time-driven consensus in multiagent networks with time delays," *IEEE Trans. Cybern.*, vol. 46, no. 5, pp. 1165–1174, May 2016.
[31] Z. Hou and S. Xiong, "On model-free adaptive control and its stability analysis," *IEEE Trans. Autom. Control*, vol. 64, no. 11, pp. 4555–4569, Nov. 2019, doi: 10.1109/TAC.2019.2894586.
[32] J. Ma, M. Ye, Y. Zheng, and Y. Zhu, "Consensus analysis of hybrid multi-agent systems: A game-theoretic approach," *Int. J. Robust Nonlinear Control*, vol. 29, no. 6, pp. 1840–1853, 2019.
[33] Y. Zhu, S. Li, J. Ma, and Y. Zheng, "Bipartite consensus in networks of agents with antagonistic interactions and quantization," *IEEE Trans. Circuits Syst. II, Exp. Briefs*, vol. 65, no. 12, pp. 2012–2016, Mar. 2018.
[34] J. Xi, C. Wang, H. Liu, and L. Wang, "Completely distributed guaranteed-performance consensualization for high-order multiagent systems with switching topologies," *IEEE Trans. Syst., Man, Cybern., Syst.*, vol. 49, no. 7, pp. 1338–1348, Jul. 2019.
[35] Q. Qi and H. Zhang, "Output feedback control and stabilization for networked control systems with packet losses," *IEEE Trans. Cybern.*, vol. 47, no. 8, pp. 2223–2234, Aug. 2017.
[36] N. Cai, C. Diao, and M. J. Khan, "A novel clustering method based on quasi-consensus motions of dynamical multiagent systems," *Complexity*, vol. 2017, Sep. 2017, Art. no. 4978613.
[37] H. Liu and H. Yu, "Decentralized state estimation for a large-scale spatially interconnected system," *ISA Trans.*, vol. 74, pp. 67–76, Mar. 2018.
[38] Y. Sun, Y. Tian, and X.-J. Xie, "Stabilization of positive switched linear systems and its application in consensus of multiagent systems," *IEEE Trans. Autom. Control*, vol. 62, no. 12, pp. 6608–6613, Dec. 2017.
[39] J. Xi, M. He, H. Liu, and J. Zheng, "Admissible output consensualization control for singular multi-agent systems with time delays," *J. Franklin Inst.*, vol. 353, no. 16, pp. 4074–4090, 2016.
[40] Z. Lu, L. Zhang, Z. Ji, and L. Wang, "Controllability of discrete-time multi-agent systems with directed topology and input delay," *Int. J. Control*. vol. 89, no. 1, pp. 179–192, 2016.
[41] Y. Chao and Z. Ji, "Necessary and sufficient conditions for multi-agent controllability of path and star topologies by exploring the information of second-order neighbors," *IMA J. Math. Control Inf.*, to be published, doi: 10.1093/imamci/dnw013.
[42] Y. Guan, Z. Ji, L. Zhang, and L. Wang, "Quadratic stabilisability of multi-agent systems under switching topologies," *Int. J. Control*, vol. 87, no. 12, pp. 2657–2668, 2014.
[43] X. Liu and Z. Ji, "Controllability of multi-agent systems based on path and cycle graphs," *Int. J. Robust Nonlinear Control*, vol. 28, no. 1, pp. 296–309, 2018.
[44] Y. Guan, Z. Ji, L. Zhang, and L. Wang, "Controllability of multi-agent systems under directed topology," *Int. J. Robust Nonlinear Control*, vol. 27, no. 18, pp. 4333–4347, Mar. 2017.
[45] S. Sundaram and C. N. Hadjicoustis, "Structural controllability and observability of linear systems over finite fields with applications to multi-agent systems," *IEEE Trans. Autom. Control*, vol. 58, no. 1, pp. 60–70, Jan. 2013.
[46] B. Liu, T. Chu, L. Wang, and G. Xie, "Controllability of a leader–follower dynamic network with switching topology," *IEEE Trans. Autom. Control*, vol. 53, no. 4, pp. 1009–1013, May 2008.
[47] Z. Ji, H. Lin, and H. Yu, "Protocols design and uncontrollable topologies construction for multi-agent networks," *IEEE Trans. Autom. Control*, vol. 60, no. 3, pp. 781–786, Mar. 2015.
[48] Z. Ji, Z. D. Wang, H. Lin, and Z. Wang, "Interconnection topologies for multi-agent coordination under leader–follower framework," *Automatica*, vol. 45, no. 12, pp. 2857–2863, 2009.
[49] Z. Ji, Z. Wang, H. Lin, and Z. Wang, "Controllability of multi-agent systems with time-delay in state and switching topology," *Int. J. Control*, vol. 83, no. 2, pp. 371–386, 2010.
[50] B. Liu, T. Chu, L. Wang, Z. Zuo, G. Chen, and H. Su, "Controllability of switching networks of multi-agent systems," *Int. J. Robust Nonlinear Control*, vol. 22, no. 6, pp. 630–644, 2012.
[51] Y. Lou and Y. Hong, "Controllability analysis of multi-agent systems with directed and weighted interconnection," *Int. J. Control*, vol. 85, no. 10, pp. 1486–1496, May 2012.
[52] M. A. Rahimian and A. G. Aghdam, "Structural controllability of multi-agent networks: Robustness against simultaneous failures," *Automatica*, vol. 49, no. 11, pp. 3149–3157, 2013.
[53] H. G. Tanner, "On the controllability of nearest neighbor interconnections," in *Proc. 43rd IEEE Conf. Decis. Control*, Dec. 2014, pp. 2467–2472.
[54] M. Ji and M. Egerstedt, "A graph theoretic characterization of controllability for multi-agent systems," in *Proc. Amer. Control Conf.*, Jul. 2007, pp. 4588–4593.
[55] Z. Yuan, C. Zhao, Z. Di, W. Wang, and Y. Lai, "Exact controllability of complex networks," *Nat. Commun.*, vol. 4, p. 2447, Sep. 2013, doi: 10.1038/ncomms3447.
[56] S. Zhang, M. K. Camlibel, and M. Cao, "Upper and lower bounds for controllable subspaces of networks of diffusively coupled agents," *IEEE Trans. Autom. Control*, vol. 59, no. 3, pp. 745–750, Mar. 2014.
[57] S. Cao, Z. Ji, H. Lin, and H. Yu, "Perfectly controllable multi-agent networks," Jul. 2018. [Online]. Available: arXiv: 1807.00479v1.

Zhijian Ji (Senior Member, IEEE) was born in 1973. He received the M.S. degree in applied mathematics from the Ocean University of China, Qingdao, China, in 1998, and the Ph.D. degree in control theory and control engineering from Peking University, Beijing, China, in 2015.

He is currently a full-time Professor of automation and electrical engineering with Qingdao University, Qingdao. In 2015 and in 2013, he was, respectively, a Visiting Professor with the University of Notre Dame, Notre Dame, IN, USA, and the University of Alberta, Edmonton, AB, Canada. From 2009 to 2010 and from 2008 to 2009, he was, respectively, a Research Fellow with the National University of Singapore, Singapore, and Brunel University London, Uxbridge, U.K. From 2006 to 2007, he was a Senior Research Associate with the City University of Hong Kong, Hong Kong. He has published more than 120 refereed papers in journals and international conference proceedings. His research interests include multiagent systems, switched control systems, networked control systems, intelligent control, and robot systems.

Prof. Ji is a member of the Technical Committee on Control Theory in China.

Hai Lin (Senior Member, IEEE) received the Ph.D. degree from the Department of Electrical Engineering, University of Notre Dame, Notre Dame, IN, USA, in 2005.

He is currently a Professor with the Department of Electrical Engineering, University of Notre Dame. He was an Assistant Professor with the National University of Singapore, Singapore, from 2006 to 2011. His teaching and research interests are in the multidisciplinary study of the problems at the intersections of control theory, formal methods, and machine learning. His current research thrust is on cyber-physical systems, multirobot cooperative tasking, human–machine collaboration, and security/privacy.

Prof. Lin is a recipient of the 2013 NSF CAREER Award. He has been served in several committees and editorial board, including the IEEE TRANSACTIONS ON AUTOMATIC CONTROL. He served as the Chair for the IEEE Control Systems Society Technical Committee on Discrete Event Systems, the Program Chair for the IEEE International Conference on Control and Automation 2011, and the IEEE Computational Intelligence Society 2011, and the Chair for the IEEE Systems, Man and Cybernetics Singapore Chapter for 2009 and 2010.

Authorized licensed use limited to: Qingdao University. Downloaded on September 27,2020 at 09:14:25 UTC from IEEE Xplore. Restrictions apply.

This article has been accepted for inclusion in a future issue of this journal. Content is final as presented, with the exception of pagination.

Shaobin Cao was born in Shanxi, China, in 1992. He received the M.S. degree from the School of Automation, Qingdao University, Qingdao, China, in 2019.

His research interests included multiagent systems and network with antagonistic interactions.

Qingyuan Qi received the B.S. degree in mathematics and the Ph.D. degree in control theory and engineering from Shandong University, Jinan, China, in 2012 and 2018, respectively.

He is currently a Lecturer with the Institute of Complexity Science, School of Automation, Qingdao University, Qingdao, China. He is also a Postdoctoral Fellow with the School of Electrical and Electronic Engineering, Nanyang Technological University, Singapore. His research interests include optimal control, optimal estimation, stabilization, and stochastic systems.

Huizi Ma received the B.S. and Ph.D. degrees from Harbin Engineering University, Harbin, China, in 2009 and 2014, respectively.

She is currently a Lecturer with the College of Mathematics and System Science, Shandong University of Science and Technology, Qingdao, China. Her research interests mainly include stochastic control and backward stochastic differential equations, and their applications in financial studies.

Authorized licensed use limited to: Qingdao University. Downloaded on September 27,2020 at 09:14:25 UTC from IEEE Xplore. Restrictions apply.